Title

JMML tumor cells disrupt normal hematopoietic stem cells by imposing inflammatory stress through overproduction of IL-1β

Journal

Blood Advances, 6(1)

ISSN

2473-9529

Authors

Yan, Yuhan
Dong, Lei
Chen, Chao
et al.

Publication Date

2022-01-11

DOI

10.1182/bloodadvances.2021005089

Peer reviewed

STIMULUS REPORT

blood advances

JMML tumor cells disrupt normal hematopoietic stem cells by imposing inflammatory stress through overproduction of IL-1β

Yuhan Yan,[1,2,*] Lei Dong,[1,*] Chao Chen,[1] Kevin D. Bunting,[1] Qianjin Li,[1] Elliot Stieglitz,[3] Mignon L. Loh,[3] and Cheng-Kui Qu[1]

[1]Department of Pediatrics, Aflac Cancer and Blood Disorders Center, Winship Cancer Institute, Children's Healthcare of Atlanta, Emory University School of Medicine, Atlanta, GA; [2]Department of Hematology, Third Xiangya Hospital, Central South University, Changsha, China; and [3]Division of Pediatric Hematology-Oncology, Department of Pediatrics, University of California at San Francisco, San Francisco, CA

Key Points

- Normal hematopoiesis is suppressed by JMML tumor cells as a result of the aberrant activation and exhaustion of stem cells.
- JMML cells impose inflammatory stress on normal stem cells by over production of IL-1β.

Development of normal blood cells is often suppressed in juvenile myelomonocytic leukemia (JMML), a myeloproliferative neoplasm (MPN) of childhood, causing complications and impacting therapeutic outcomes. However, the mechanism underlying this phenomenon remains uncharacterized. To address this question, we induced the most common mutation identified in JMML (*Ptpn11*^{E76K}) specifically in the myeloid lineage with hematopoietic stem cells (HSCs) spared. These mice uniformly developed a JMML-like MPN. Importantly, HSCs in the same bone marrow (BM) microenvironment were aberrantly activated and differentiated at the expense of self-renewal. As a result, HSCs lost quiescence and became exhausted. A similar result was observed in wild-type (WT) donor HSCs when co-transplanted with *Ptpn11*$^{E76K/+}$ BM cells into WT mice. Co-culture testing demonstrated that JMML/MPN cells robustly accelerated differentiation in mouse and human normal hematopoietic stem/progenitor cells. Cytokine profiling revealed that *Ptpn11*$^{E76K/+}$ MPN cells produced excessive IL-1β, but not IL-6, T NF-α, IFN-γ, IL-1α, or other inflammatory cytokines. Depletion of the IL-1β receptor effectively restored HSC quiescence, normalized their pool size, and rescued them from exhaustion in *Ptpn11*$^{E76K/+/IL\text{-}1R-/-}$ double mutant mice. These findings suggest IL-1β signaling as a potential therapeutic target for preserving normal hematopoietic development in JMML.

Introduction

Juvenile myelomonocytic leukemia (JMML), a clonal hematological malignancy, is an aggressive myeloproliferative neoplasm (MPN) of childhood. It is characterized by hypersensitivity of myeloid progenitors to cytokines granulocyte-macrophage colony-stimulating factor and interleukin-3 (IL-3)[1-3] and excessive production of mutant myeloid cells and monocytes with maturation. This malignancy is associated with genetic mutations in the signaling proteins involved in the Ras/Erk pathway,[4-6] among which protein tyrosine phosphatase *PTPN11* (SHP2), a positive regulator of Ras signaling,[7,8] is most frequently mutated (~35%).[9,10] The pathophysiology of this disease remains incompletely understood because of its rarity. Normal hematopoietic cell development is often suppressed or impaired in JMML, causing complications and affecting overall therapeutic outcomes. However, the underlying mechanism has not been addressed. Our laboratory previously generated an inducible mouse model of JMML with the *Ptpn11*^{E76K} mutation,[11,12] the most common mutation identified in JMML.[9,10] Using this unique conditional

Submitted 26 April 2021; accepted 20 July 2021; prepublished online on *Blood Advances* First Edition 23 September 2021; final version published online 7 January 2022. DOI 10.1182/bloodadvances.2021005089.

*Y.Y. and L.D. contributed equally to this study.

The full-text version of this article contains a data supplement.

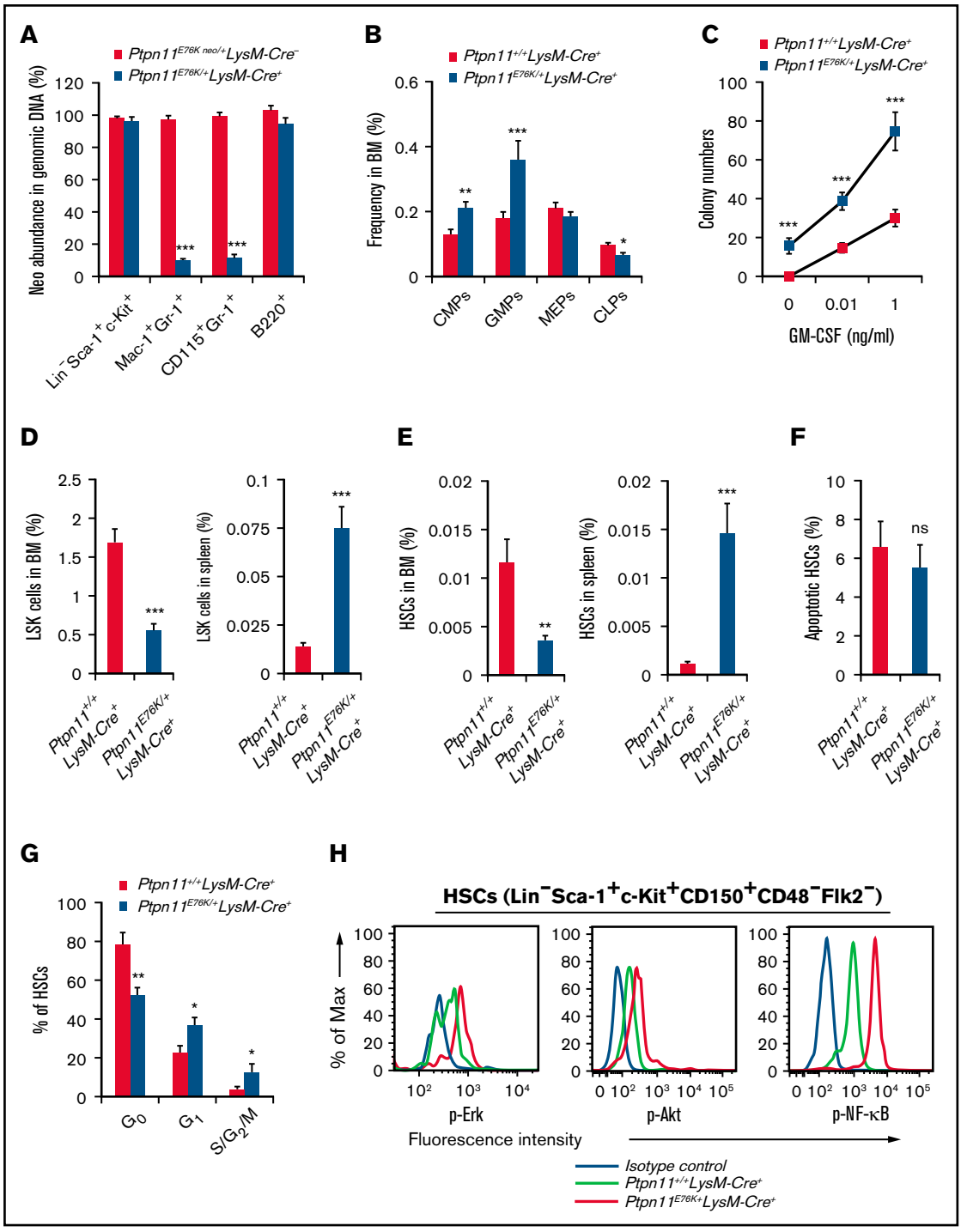

Figure 1. Normal HSCs are aberrantly activated by *Ptpn11*$^{E76K/+}$ neoplastic cells, leading to accelerated differentiation and exhaustion. (A) Genomic DNA was extracted from LSK cells (Lin$^-$Sca-1$^+$c-Kit$^+$), myeloid cells (Mac-1$^+$Gr-1$^+$), monocytes (CD115$^+$Gr-1$^+$), and B cells (B220$^+$) isolated from the BM of *Ptpn11*$^{E76K/+}$*LysM-Cre*$^+$ mice and *Ptpn11*$^{+/+}$*LysM-Cre*$^+$ littermates. The abundance of the inhibitory neo cassette with a stop codon in the targeted *Ptpn11* allele was determined by quantitative polymerase chain reaction (n = 5 mice per genotype). (B) BM cells harvested from 5- to 6-month-old *Ptpn11*$^{E76K/+}$*LysM-Cre*$^+$ mice and *Ptpn11*$^{+/+}$*LysM-Cre*$^+$ littermates were assayed for the frequencies of common myeloid progenitors (CMPs), granulocyte macrophage progenitors (GMPs), megakaryocyte erythroid progenitors (MEPs), and common lymphoid progenitors (CLPs; n = 6 mice per genotype). (C) BM cells (2×10^4 cells) collected from 5- to 6-month-old *Ptpn11*$^{E76K/+}$*LysM-Cre*$^+$ mice and *Ptpn11*$^{+/+}$*LysM-Cre*$^+$ littermates (n = 3 mice per genotype) were processed for colony-forming unit assays. (D-E) Frequencies of HSC-enriched LSK (Lin$^-$Sca-1$^+$c-Kit$^+$) cells (D) and HSCs (Lin$^-$Sca-1$^+$c-Kit$^+$CD150$^+$CD48$^-$Flk2$^-$) (E) in the BM and spleens of 5- to 6-month-old *Ptpn11*$^{E76K/+}$*LysM-Cre*$^+$ mice and *Ptpn11*$^{+/+}$*LysM-Cre*$^+$ littermates (n = 6 mice per genotype) were determined by multiparameter fluorescence-activated cell sorting (FACS) analyses. (F-H) BM cells freshly isolated from *Ptpn11*$^{E76K/+}$*LysM-Cre*$^+$ mice and *Ptpn11*$^{+/+}$*LysM-Cre*$^+$ littermates were assayed by FACS analyses to determine apoptotic cells (n = 6 mice per genotype) (F), cell cycle distribution (n = 5 mice per

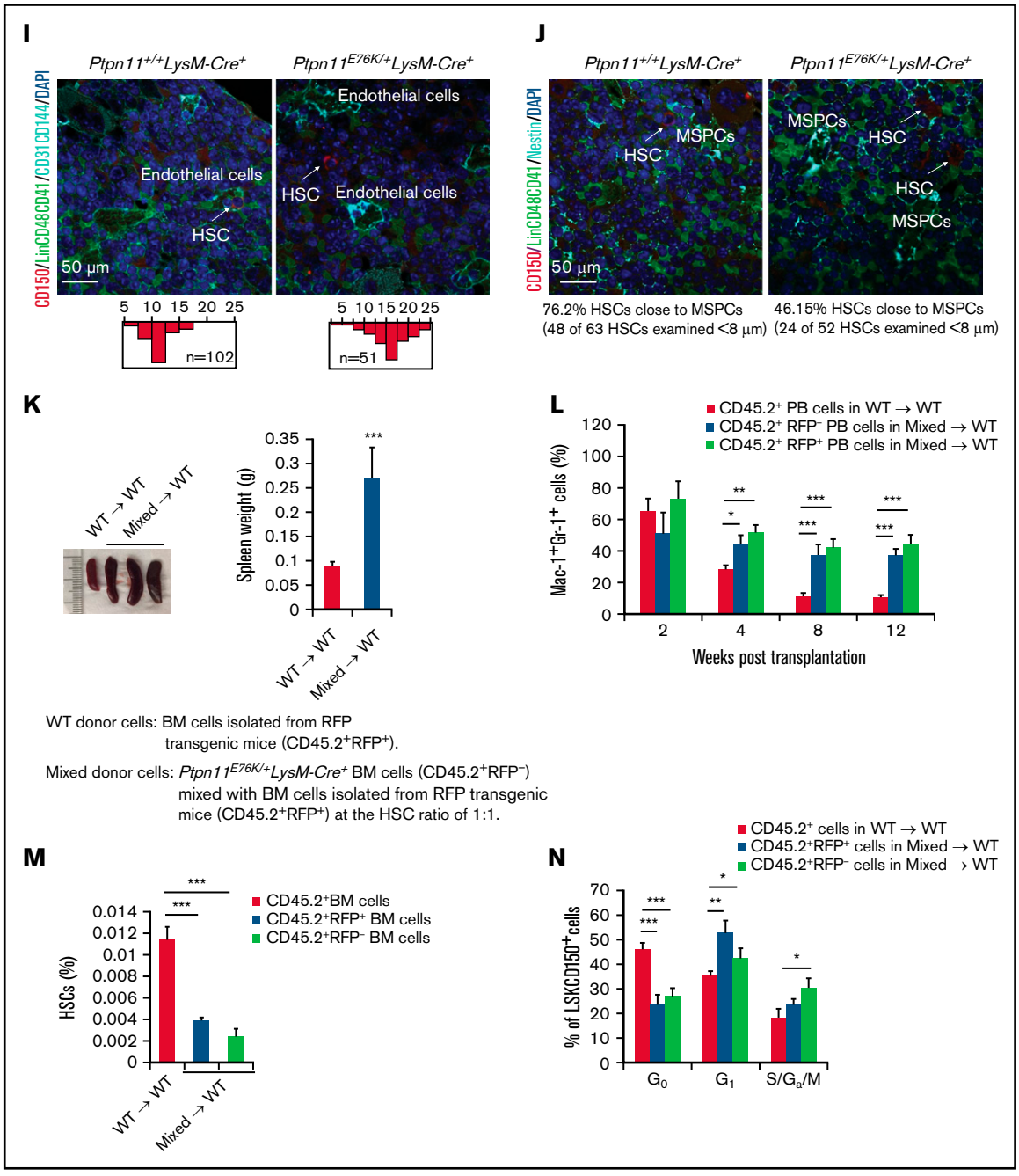

Figure 1. (continued) genotype) (G), and levels of phosphorylated Erk (p-Erk), p-Akt, and p-NF-κB in HSCs (n = 4 mice per genotype) (H). (I-J) Bone sections prepared from 4- to 6-month-old *Ptpn11*$^{E76K/+}$*LysM-Cre*$^{+}$ mice and *Ptpn11*$^{+/+}$*LysM-Cre*$^{+}$ littermates were processed for immunofluorescence staining with the indicated antibodies. Spatial relationship between HSCs (Lin^{-}CD48^{-}CD41^{-}CD150^{+}) and endothelial (CD31^{+}CD144^{+}) cells was examined (representative images from n = 5 mice per genotype are shown); the distance of these 2 types of cells was calculated (I). Spatial relationship between HSCs (Lin^{-}CD48^{-}CD41^{-}CD150^{+}) and mesenchymal stem progenitor cells (MSPCs; Nestin^{+}) was examined (representative images from n = 6 mice per genotype are shown); HSCs within 8 μm of MSPCs were considered to be close to MSPCs (J). (K-N) BM cells harvested from 3-month-old *Ptpn11*$^{E76K/+}$*LysM-Cre*$^{+}$ mice (CD45.2^{+}RFP^{-}) and WT RPF transgenic mice (CD45.2^{+}RFP^{+}) were mixed at the HSC ratio of 1:1. The mixed BM cells and BM cells isolated from WT RPF transgenic mice (CD45.2^{+}RFP^{+}) were transplanted IV into lethally irradiated WT BoyJ mice (CD45.1^{+}; n = 8 and 6 mice for mixed BM cells and WT BM cells, respectively). Sixteen weeks after transplantation, recipient mice were euthanized. Spleen weights (normalized against body weights) were documented (K). Frequencies of Mac-1^{+}Gr-1^{+} cells in different donor-derived subpopulations in the peripheral blood (PB) were examined at the indicated time points (L). The pool sizes of HSCs (Lin^{-}Sca-1^{+}c-Kit^{+}CD150^{+}CD48^{-}) (M) and the cell cycle distribution of HSCs (Lin^{-}Sca-1^{+} c-Kit^{+}CD150^{+}) in different donor-derived populations (N) were determined at 16 weeks after transplantation as above. **P* = .05, ***P* = .01, ****P* = .001. DAPI, 4′, 6-diamidino-2-phenylindole; GM-CSF, granulocyte-macrophage colony-stimulating factor; ns, not significant.

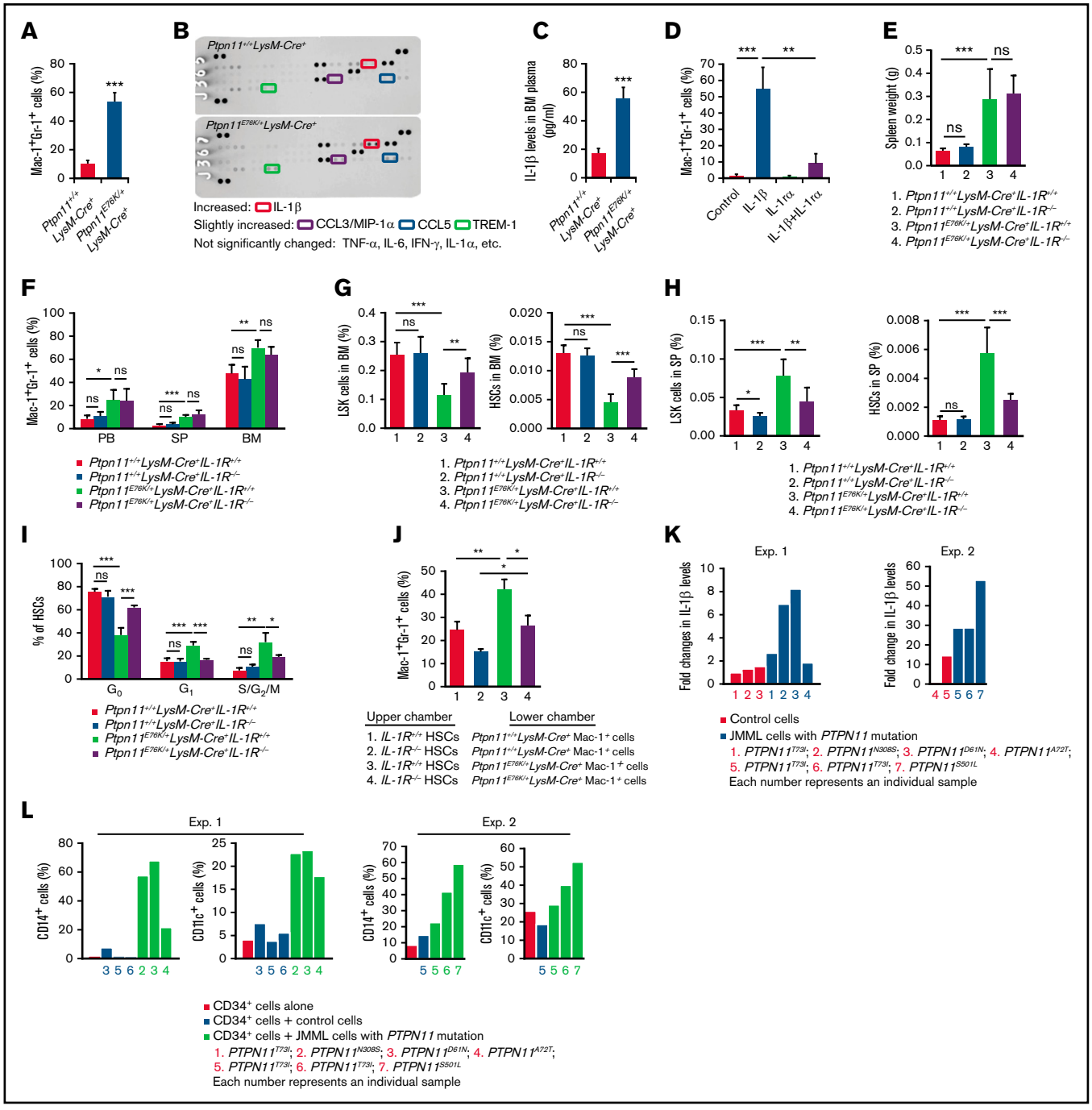

Figure 2. JMML cells produce excessive IL-1β that plays a key role in driving HSC attrition. (A) Purified WT HSCs ($Lin^-Sca\text{-}1^+c\text{-}Kit^+CD150^+CD48^-Flk2^-$) were cocultured with BM cells isolated from *Ptpn11*$^{E76K/+}$*LysM-Cre*$^+$ and *Ptpn11*$^{+/+}$*LysM-Cre*$^+$ mice in 2-chamber transwell systems in StemSpan medium supplemented with thrombopoietin (TPO; 50 ng/mL), Flt3 ligand (50 ng/mL), and stem cell factor (SCF; 50 ng/mL) for 8 days. Percentages of $Mac\text{-}1^+Gr\text{-}1^+$ cells derived from HSCs were determined. Experiments were performed 3 times, and similar results were obtained in each. Results shown are the mean ± standard deviation (SD) of triplicates from 1 experiment. (B-C) BM plasma collected from 16-week-old *Ptpn11*$^{E76K/+}$*LysM-Cre*$^+$ mice and *Ptpn11*$^{+/+}$*LysM-Cre*$^+$ control mice (n = 3 mice per genotype) were processed for chemokine-cytokine array analyses. Representative results from 1 pair of the mice are shown (B). Levels of IL-1β in the BM plasma were quantified by enzyme-linked immunosorbent assay (n = 5 mice per genotype) (C). (D) WT HSCs ($Lin^-Sca\text{-}1^+c\text{-}Kit^+CD150^+CD48^-$) were cultured in StemSpan medium supplemented with TPO (100 ng/mL), Flt3 ligand (50 ng/mL), and SCF (100 ng/mL) in the presence or absence of IL-1β (10 ng/mL) and/or IL-1rα (10 ng/mL). Frequencies of $Mac\text{-}1^+Gr\text{-}1^+$ cells were determined 7 days later. (E-I) *Ptpn11*$^{+/+}$*LysM-Cre*$^+$*IL-1R*$^{+/+}$, *Ptpn11*$^{+/+}$*LysM-Cre*$^+$*IL-1R*$^{-/-}$, *Ptpn11*$^{E76K/+}$*LysM-Cre*$^+$*IL-1R*$^{+/+}$, and *Ptpn11*$^{E76K/+}$*LysM-Cre*$^+$*IL-1R*$^{-/-}$ mice were generated and euthanized at the age of 4 months. Spleen weights (normalized against body weights) were documented (n = 8-9 mice per genotype) (E). Percentages of $Mac\text{-}1^+Gr\text{-}1^+$ cells in the peripheral blood, spleen, and BM were determined (n = 4-7 mice per genotype) (F). Frequencies of LSK cells and HSCs ($Lin^-Sca\text{-}1^+c\text{-}Kit^+CD150^+CD48^-$) in the BM (n = 7-10 mice per genotype) (G) and in the spleen (n = 6-10 mice per genotype) (H) and the cell cycle distribution in HSCs ($Lin^-Sca\text{-}1^+c\text{-}Kit^+CD150^+CD48^-$) in the BM (n = 4 mice per genotype) (I) were determined by multiparameter FACS analyses. (J) Purified HSCs ($Lin^-Sca\text{-}1^+$

Ptpn11^{E76K} allele, in the present study we have determined the cellular and molecular mechanisms by which normal blood cell development is disrupted in JMML.

Materials and methods

Materials and methods are described in detail in the data supplement.

Mixed BM cell transplantation assays

Bone marrow (BM) cells collected from *Ptpn11*$^{E76K/+}$*LysM-Cre*$^{+}$ mice (CD45.2^{+}RFP^{-}) were mixed with BM cells isolated from wild-type (WT) red fluorescent protein (RFP) transgenic mice (CD45.2^{+}RFP^{+}) at the hematopoietic stem cell (HSC) ratio of 1:1. The mixed cells were then transplanted into lethally irradiated (1100 cGy) BoyJ mice (CD45.1^{+}) by tail vein injection. Hematopoietic cell reconstitution, HSC pool size, and HSC cycling status in the recipient mice were determined by multiparameter fluorescence-activated cell sorting analyses. The donor cell origins of the reconstituted hematopoietic cells were distinguished on the basis of the expression of the isoforms of CD45 and the expression of RFP. In addition, the recipient mice were monitored for MPN development.

Results and discussion

Normal HSCs are aberrantly activated in JMML, leading to accelerated differentiation and exhaustion

In an effort to determine the mechanism by which leukemic cells affect normal blood cell development in JMML, we generated myeloid lineage-specific *Ptpn11*^{E76K} knock-in mice (*Ptpn11*$^{E76K/+}$*LysM-Cre*$^{+}$) by crossing *Ptpn11*^{E76K} conditional mice (*Ptpn11*$^{E76K\ neo/+}$)[11] with *LysM-Cre*$^{+}$ transgenic mice, which express Cre DNA recombinase specifically in myeloid cells.[13] Because of the cell autonomous effects of the *Ptpn11*^{E76K} mutation, *Ptpn11*$^{E76K/+}$*LysM-Cre*$^{+}$ mice (both males and females) uniformly developed a profound JMML-like MPN at the age of 4 to 6 weeks, as evidenced by splenomegaly and increased myeloid cells (Mac-1^{+}Gr-1^{+}) and inflammatory monocytes (CD115^{+}Gr-1^{+}) in the BM, spleen, liver, and lung (supplemental Figure 1A-C), whereas lymphoid cells (T and B cells) were decreased (supplemental Figure 1D). Histopathological examination revealed hyperproliferation of myeloid cells in the BM/spleen and extensive myeloid cell infiltration in nonhematopoietic tissues (supplemental Figure 1E). As a result, 80% of these animals died within 12 months. Genotyping analyses showed that the *LoxP*-flanked neo cassette with a stop codon, which inactivated the targeted *Ptpn11*$^{E76K\ Neo}$ allele,[11] was deleted in 90% to 95% of Mac-1^{+}Gr-1^{+} myeloid cells and CD115^{+}Gr-1^{+} monocytes, but not in stem cell–enriched Lin^{-}Sca-1^{+}c-Kit^{+} (LSK) cells or lymphoid cells in *Ptpn11*$^{E76K/+}$*LysM-Cre*$^{+}$ mice (Figure 1A), verifying that the *Ptpn11*$^{E76K/+}$ mutation was indeed restricted to myeloid cells. Common myeloid progenitors and granulocyte macrophage progenitors were increased (however, megakaryocyte erythroid progenitors were not significantly changed), whereas common lymphoid progenitors were decreased in *Ptpn11*$^{E76K/+}$*LysM-Cre*$^{+}$ mice (Figure 1B). Consistent with these phenotypic data, functional myeloid progenitors in *Ptpn11*$^{E76K/+}$*LysM-Cre*$^{+}$ mice demonstrated enhanced sensitivity to granulocyte-macrophage colony-stimulating factor in colony-forming unit assays (Figure 1C), a characteristic feature of JMML. Imaging analyses illustrated that myeloid cells in the BM (supplemental Figure 2A) and the red pulp of the spleen (supplemental Figure 2B) were highly proliferative in *Ptpn11*$^{E76K/+}$*LysM-Cre*$^{+}$ mice, as demonstrated by substantially increased Ki67^{+} cells in these tissues.

Interestingly, LSK cells that were free of the *Ptpn11*^{E76K} mutation (Figure 1A) in the BM were decreased by more than threefold in *Ptpn11*$^{E76K/+}$*LysM-Cre*$^{+}$ mice (Figure 1D). LSK cells in the spleen were markedly increased (Figure 1D), indicative of extramedullary hematopoiesis. Moreover, HSCs (Lin^{-}Sca-1^{+}c-Kit^{+}CD150^{+}CD48^{-}Flk2^{-}) in the BM and spleen were also greatly decreased and increased, respectively, in these animals (Figure 1E; supplemental Figure 1F). Apoptosis in HSCs in *Ptpn11*$^{E76K/+}$*LysM-Cre*$^{+}$ mice was comparable to that in control littermates (Figure 1F). Cell cycle analyses revealed that HSCs in *Ptpn11*$^{E76K/+}$*LysM-Cre*$^{+}$ mice were cycling faster than those in WT littermates (Figure 1G). These data together suggest that the decrease in HSCs in *Ptpn11*$^{E76K/+}$*LysM-Cre*$^{+}$ mice was due to aberrant activation and loss of dormancy. Indeed, intracellular signaling activities (Erk, Akt, and NF-κB), especially NF-κB signaling, were increased in HSCs in *Ptpn11*$^{E76K/+}$*LysM-Cre*$^{+}$ mice compared with those in control animals (Figure 1H).

Consistent with the elevated cell cycling status, HSCs in *Ptpn11*$^{E76K/+}$*LysM-Cre*$^{+}$ mice were displaced from the endothelial and mesenchymal stem progenitor cell niches that maintain HSCs in dormancy.[14-17] The distance of HSCs to CD31^{+}CD144^{+} endothelial niche cells increased from ~11 to ~16 μm (Figure 1I), and only 46% of HSCs in *Ptpn11*$^{E76K/+}$*LysM-Cre*$^{+}$ BM as opposed to 76% in controls were close to Nestin^{+} mesenchymal stem progenitor cell niches (Figure 1J). Given that the *Ptpn11* mutant allele was not activated in HSCs in *Ptpn11*$^{E76K/+}$*LysM-Cre*$^{+}$ mice, these data suggest that the cues that forced HSCs to enter the cell cycle were from the extracellular microenvironment.

To further test this hypothesis, we collected BM cells from *Ptpn11*$^{E76K/+}$*LysM-Cre*$^{+}$ mice (CD45.2^{+}), mixed them with WT

Figure 2. (continued) c-Kit^{+}CD150^{+}CD48^{-}) from WT and *IL-1R*$^{-/-}$ mice were cocultured with Mac-1^{+} cells isolated from 4-month-old *Ptpn11*$^{+/+}$*LysM-Cre*$^{+}$ and *Ptpn11*$^{E76K/+}$*LysM-Cre*$^{+}$ mice in StemSpan medium supplemented with TPO (100 ng/mL), Flt3 ligand (50 ng/mL), and SCF (100 ng/mL) in a 2-chamber transwell system for 8 days. Frequencies of Mac-1^{+}Gr-1^{+} cells differentiated from HSCs in the upper chamber were assayed by FACS analyses. Experiments were performed 3 times, and similar results were obtained in each. Results shown are mean ± SD of triplicates from 1 experiment. (K) Cells from patients with JMML carrying *PTPN11* mutations and healthy BM cells were cultured in StemSpan medium (serum free) supplemented with human SCF (hSCF; 50 ng/mL), hTPO (50 ng/mL), and hFlt3 ligand (50 ng/mL) for 3 days (experiment 1 [Exp. 1] and Exp 2). Culture medium was collected and analyzed for IL-1β by FACS with IL-1β antibody–conjugated beads. (L) CD34^{+} cord blood cells were isolated and cocultured with cells from patients with JMML or control cells in transwell systems in StemSpan medium (serum free) supplemented with hSCF (50 ng/mL), hTPO (50 ng/mL), and hFlt3 ligand (50 ng/mL). Five days (Exp. 1) or 12 days (Exp. 2) later, percentages of CD14^{+} cells and CD11c^{+} cells differentiated from CD34^{+} cells were determined by FACS analyses. *P = .05, **P = .01, ***P = .001. IFN-γ, interferon-γ; ns, not significant; TNF-α, tumor necrosis factor α.

BM cells isolated from WT RFP transgenic mice ($CD45.2^+RFP^+$) at the HSC ratio of 1:1, and transplanted the mixed cells into lethally irradiated WT BoyJ mice ($CD45.1^+$). The hematopoietic system was fully reconstituted by donor cells, as evidenced by ~100% $CD45.2^+$ cells in the peripheral blood (supplemental Figure 3A). All recipient mice developed an MPN (supplemental Figure 3B) and exhibited splenomegaly (Figure 1K). Notably, Mac-1^+Gr-1^+ myeloid cells derived from both *Ptpn11*$^{E76K/+}$*LysM-Cre*$^+$ donor cells ($RFP^-CD45.2^+$) and WT ($RFP^+CD45.2^+$) donor cells were increased (Figure 1L; supplemental Figure 3C). Moreover, HSCs in both *Ptpn11*$^{E76K/+}$*LysM-Cre*$^+$ donor cell– and WT donor cell–reconstituted BM cell populations decreased (Figure 1M) and displayed hyperactivation and loss of quiescence (Figure 1N). The fact that HSCs of *Ptpn11*$^{E76K/+}$*LysM-Cre*$^+$ donor origin and those of WT donor origin were equally hyperactivated in the same diseased recipient mice strongly suggests that the deleterious effects on stem cells were from MPN cells.

JMML cells produce excessive IL-1β that plays a key role in driving HSC exhaustion

To identify the mechanism by which HSCs are aberrantly activated in *Ptpn11*$^{E76K/+}$*LysM-Cre*$^+$ mice, we cocultured purified HSCs with MPN cells in 2 separate chambers that still allowed soluble factors to freely cross. Compared with control cells, *Ptpn11*$^{E76K/+}$*LysM-Cre*$^+$ MPN cells markedly enhanced HSC differentiation toward myeloid cells, even in the stem cell maintenance medium (Figure 2A). Cytokine-chemokine array analyses for the BM plasma from *Ptpn11*$^{E76K/+}$*LysM-Cre*$^+$ mice revealed that among the 40 cytokines, chemokines, and acute phage proteins examined, the proinflammatory cytokine IL-1β was increased (Figure 2B). However, no differences in the levels of other inflammatory cytokines such as tumor necrosis factor α, IL-6, interferon-γ, or IL-1α were detected. IL-1β levels in the BM plasma of *Ptpn11*$^{E76K/+}$*LysM-Cre*$^+$ mice were tripled compared with those in *Ptpn11*$^{+/+}$*LysM-Cre*$^+$ mice by enzyme-linked immunosorbent assay (Figure 2C). Indeed, HSCs cultured with recombinant IL-1β in the stem cell maintenance medium differentiated robustly toward myeloid cells, and this effect was abolished by the addition of the IL-1 receptor antagonist IL-1ra (Figure 2D).

To further verify the role of IL-1β in mediating the effects of MPN cells on normal stem cells, we generated *Ptpn11*$^{E76K/+}$*LysM-Cre*$^+$*IL-1R*$^{-/-}$ double-mutant mice by crossing *Ptpn11*$^{E76K/+}$*LysM-Cre*$^+$ mice with *IL-1R*$^{+/-}$ mice[18] and examined HSCs in these mice. Because of the activation of the *Ptpn11*^{E76K} mutant allele in myeloid cells, the double-mutant mice still developed an MPN (Figure 2E-F), whereas T and B cells were decreased (supplemental Figure 4A-B), suggesting that the autocrine effects of IL-1β on MPNs were minimal compared with the cell-intrinsic effects of the *Ptpn11*$^{E76K/+}$ mutation. Importantly, however, LSK cells and HSCs in *Ptpn11*$^{E76K/+}$*LysM-Cre*$^+$*IL-1R*$^{-/-}$ double-mutant mice were largely rescued (Figure 2G; supplemental Figure 4C). Moreover, extramedullary hematopoiesis was corrected, because LSK cells and HSCs in the spleen in double-mutant mice were significantly reduced (Figure 2H; supplemental Figure 4D). The cell cycling status and quiescence of LSK cells and HSCs in the double-mutant mice were restored (Figure 2I; supplemental Figure 4E). Indeed, the activating effects of *Ptpn11*$^{E76K/+}$*LysM-Cre*$^+$ MPN cells (Mac-1^+) on *IL-1R*$^{-/-}$ HSCs were abolished in coculture testing (Figure 2J). Finally, we assessed IL-1β production in primary cells of patients with JMML with *PTPN11* mutations. Overall, *PTPN11*-mutated JMML cells produced much higher levels of IL-1β (Figure 2K). Moreover, compared with normal human BM cells, patient cells accelerated differentiation of cord blood $CD34^+$ stem/progenitor cells toward $CD14^+$ myelomonocytes and $CD11c^+$ cells in the stem cell maintenance medium (Figure 2L), reaffirming the deleterious effects of JMML tumor cells on normal stem cells. Taken together, the data presented in this report suggest that targeting IL-1β signaling may preserve normal hematopoietic cell development in JMML. This is especially important given that the IL-1 receptor is dispensable for steady state hematopoiesis[19] and that IL-1β inhibitors, such as anakinra, are in common use for inflammatory conditions of childhood.

Acknowledgments

The authors thank Emory Integrated Cellular Imaging and Pediatrics/Winship Flow Cytometry shared resources for technical support and the Aflac Cancer and Blood Disorders Center Biorepository for patient specimens.

This work was supported by National Heart, Lung, and Blood Institute grant HL130995 and National Cancer Institute grant CA255831 (C.-K.Q.) and a Winship Cancer Institute Invest$ Pilot grant (C.K.Q.). Y.Y. is a visiting student of the Emory University School of Medicine–Xiangya Hospital Exchange Program. M.L.L. is the Benioff Chair of Children's Health and the Deborah and Arthur Ablin Endowed Chair for Pediatric Molecular Oncology at Benioff Children's Hospital.

Authorship

Contribution: Y.Y., L.D., C.C., and Q.L. conducted the research and summarized the data; K.D.B., E.S., and M.L.L. provided critical materials and advice and discussed the work; C.-K.Q. designed experiments and directed the entire study; and Y.Y. and C.-K.Q. wrote the manuscript, with input from the other authors.

Conflict-of-interest disclosure: The authors declare no competing financial interests.

ORCID profiles: C.C., 0000-0001-9526-0099; E.S., 0000-0001-7032-4623; M.L.L., 0000-0003-4099-4700; C.-K.Q., 0000-0002-4256-8652.

Correspondence: Cheng-Kui Qu, Department of Pediatrics, Aflac Cancer and Blood Disorders Center, Children's Healthcare of Atlanta, Winship Cancer Institute, Emory University School of Medicine, 1760 Haygood Drive NE, HSRB E302, Atlanta, GA 30322; e-mail: cheng-kui.qu@emory.edu.

References

1. Birnbaum RA, O'Marcaigh A, Wardak Z, et al. Nf1 and Gmcsf interact in myeloid leukemogenesis. *Mol Cell.* 2000;5(1):189-195.
2. Emanuel PD, Bates LJ, Castleberry RP, Gualtieri RJ, Zuckerman KS. Selective hypersensitivity to granulocyte-macrophage colony-stimulating factor by juvenile chronic myeloid leukemia hematopoietic progenitors. *Blood.* 1991;77(5):925-929.
3. Yu WM, Daino H, Chen J, Bunting KD, Qu CK. Effects of a leukemia-associated gain-of-function mutation of SHP-2 phosphatase on interleukin-3 signaling. *J Biol Chem.* 2006;281(9):5426-5434.
4. Chang TY, Dvorak CC, Loh ML. Bedside to bench in juvenile myelomonocytic leukemia: insights into leukemogenesis from a rare pediatric leukemia. *Blood.* 2014;124(16):2487-2497.
5. Emanuel PD. Juvenile myelomonocytic leukemia and chronic myelomonocytic leukemia. *Leukemia.* 2008;22(7):1335-1342.
6. Liu X, Sabnis H, Bunting KD, Qu CK. Molecular targets for the treatment of juvenile myelomonocytic leukemia. *Adv Hematol.* 2012;2012:308252.
7. Qu CK. Role of the SHP-2 tyrosine phosphatase in cytokine-induced signaling and cellular response. *Biochim Biophys Acta.* 2002;1592(3):297-301.
8. Mohi MG, Neel BG. The role of Shp2 (PTPN11) in cancer. *Curr Opin Genet Dev.* 2007;17(1):23-30.
9. Loh ML, Vattikuti S, Schubbert S, et al. Mutations in PTPN11 implicate the SHP-2 phosphatase in leukemogenesis. *Blood.* 2004;103(6):2325-2331.
10. Tartaglia M, Niemeyer CM, Fragale A, et al. Somatic mutations in PTPN11 in juvenile myelomonocytic leukemia, myelodysplastic syndromes and acute myeloid leukemia. *Nat Genet.* 2003;34(2):148-150.
11. Xu D, Liu X, Yu WM, et al. Non-lineage/stage-restricted effects of a gain-of-function mutation in tyrosine phosphatase Ptpn11 (Shp2) on malignant transformation of hematopoietic cells. *J Exp Med.* 2011;208(10):1977-1988.
12. Dong L, Yu WM, Zheng H, et al. Leukaemogenic effects of Ptpn11 activating mutations in the stem cell microenvironment. *Nature.* 2016;539(7628):304-308.
13. Clausen BE, Burkhardt C, Reith W, Renkawitz R, Förster I. Conditional gene targeting in macrophages and granulocytes using LysMcre mice. *Transgenic Res.* 1999;8(4):265-277.
14. Ding L, Saunders TL, Enikolopov G, Morrison SJ. Endothelial and perivascular cells maintain haematopoietic stem cells. *Nature.* 2012;481(7382):457-462.
15. Kiel MJ, Yilmaz OH, Iwashita T, Yilmaz OH, Terhorst C, Morrison SJ. SLAM family receptors distinguish hematopoietic stem and progenitor cells and reveal endothelial niches for stem cells. *Cell.* 2005;121(7):1109-1121.
16. Kunisaki Y, Bruns I, Scheiermann C, et al. Arteriolar niches maintain haematopoietic stem cell quiescence. *Nature.* 2013;502(7473):637-643.
17. Méndez-Ferrer S, Michurina TV, Ferraro F, et al. Mesenchymal and haematopoietic stem cells form a unique bone marrow niche. *Nature.* 2010;466(7308):829-834.
18. Labow M, Shuster D, Zetterstrom M, et al. Absence of IL-1 signaling and reduced inflammatory response in IL-1 type I receptor-deficient mice. *J Immunol.* 1997;159(5):2452-2461.
19. Glaccum MB, Stocking KL, Charrier K, et al. Phenotypic and functional characterization of mice that lack the type I receptor for IL-1. *J Immunol.* 1997;159(7):3364-3371.